Semicond. Sci. Technol. **12** (1997) 284–290. Printed in the UK PII: S0268-1242(97)77703-4

Metastable hole traps in high-resistivity silicon

Berit Sundby Avset†

Department of Physics, University of Oslo, PO Box 1048 Blindern, N-0316 Oslo, Norway

Received 9 September 1996, accepted for publication 21 November 1996

Abstract. A new metastable peak due to hole traps has been observed in DLTS measurements on as-processed diodes of high-resistivity floatzone silicon. The peak consists of one or more defects which are transferred to a metastable state in an applied electric field across the pn junction, and the fraction of the defects in the metastable state depends on the field strength. The defect density has a peak between 50 and 100 μm from the junction and small densities closer to and further from the junction. It is suggested that the defects arise from diffusing impurities which react with precipitates at the edge of a denuded zone.

1. Introduction

Impurities and defects in semiconductors may give rise to energy levels in the forbidden bandgap. In some cases a defect can have more than one structural configuration in the lattice and such states are said to be metastable. If the configuration of a metastable state can be altered by varying the measurement parameters or the pre-measurement conditions the metastability can be revealed by deep-level transient spectroscopy (DLTS) measurements. The investigation of metastability in semiconductors was intensified in the mid-1980s when it was discovered that different DLTS spectra were observed when semiconductor samples were cooled with and without bias before DLTS measurements [1, 2]. Defects which are well known to exhibit metastability in silicon are phosphorus–carbon (P_sC_i) [3–6], carbon–arsenic (C_iAs_s) [6], carbon–antimony (C_iSb_s) [6] and carbon–carbon (C_iC_s) [7, 8], which are formed after irradiation and annealing of the carbon interstitial. Other examples of metastable defects with known identity are the iron–acceptor pairs [2, 9, 10].

We have found metastable hole traps in as-processed diodes made on high-resistivity floatzone silicon. The metastability was revealed in DLTS measurements where a new peak emerged in the spectra after repeated DLTS scans. We will describe the samples and the DLTS measurements in the next section, while section 3 describes and discusses the results obtained in the DLTS measurements.

2. Materials and methods

2.1. Silicon diode preparation

In this investigation we used diodes made on high-resistivity phosphorus-doped floatzone silicon with ⟨111⟩ orientation of the crystal. The substrates had two different doping concentrations which were determined by CV measurements on the diodes after processing [11]. The diode NN2-1 had an effective doping concentration of 2.5×10^{12} cm^{-3} while WD3-1 had 8×10^{11} cm^{-3}. The main processing steps are summarized in table 1.

Table 1. Processing steps.

1	Oxidation, 1100 °C
2	Removal of oxide from backside
3	Gas-phase phosphorus deposition on backside, 1100 °C
4	Phosphorus diffusion and oxidation, 1000 °C
5	Photoprocess for pn junction
6	Gas-phase boron deposition on frontside, 970 °C
7	Boron diffusion and oxidation, 1000 °C
8	Segregation annealing, 800 + 600 °C
9	Photoprocess for contact holes and removal of oxide from backside
10	Metallization on both sides
11	Photoprocess for metal pattern on frontside
12	Metal sintering

The diodes were circular with a diameter of 2.5 mm (pn junction) and had no guard ring. A 15 μm wide contact area was made inside the circumference of the diode with 25 μm wide aluminium on top. The diodes have four bonding pads for contacting the p-side of the diode.

The measurement samples were prepared by taking one diode from each wafer and mounting it on a piece of ceramic with one small and one large gold pad. The diode was glued to the large pad with silver epoxy and a gold wire was bonded between the metal on the p-side junction and the small pad.

† Now at: SINTEF Electronics and Cybernetics, PO Box 124 Blindern, N-0314 Oslo, Norway.

0268-1242/97/030284+07$19.50

2.2. DLTS measurements

Deep-level transient spectroscopy (DLTS) [12, 13] measurements were performed to detect defects with energy levels in the bandgap. We used a commercially available system from BioRad [14], DL4600, which included a sample holder cryostat with liquid nitrogen cooling. The measurement sample was adhered to the cold finger in the DLTS cryostat with silver paint and two gold-coated needles were used to contact the gold pads.

Two different measurement methods have to be employed to measure defects with energy levels in the upper and lower halves of the bandgap, the electron traps and the hole traps respectively. The electron traps are filled and emptied by varying the reverse bias voltage. The hole traps were filled by injecting holes across the pn junction by forward biasing the diode during the filling period. A high forward bias was needed and we used 2–2.5 V forward bias. The hole trap measurements were performed with various reverse biases, a 100 μs long filling pulse and an emission rate of 200 s^{-1}.

The computer program controlling the measurements can be set up to perform seven DLTS temperature scans continuously after each other. When the first scan was performed with decreasing temperature the next was with increasing temperature and so on. We scanned the diodes between 300 and 90 K, and in some measurement series we temporarily halted the program and changed the reverse bias voltage. This was always done at 90 K, based on an assumption that the thermal energy in the diodes would be too low for changes in the defect state configurations to take place at this temperature.

In the DLTS measurement the defects are detected by measuring the change in capacitance as the energy levels are emptied by carrier emission. For electron traps this results in a positive ΔC while ΔC is negative for hole traps. During the forward bias filling pulse electrons will be available as well as holes and the electron traps will be filled to some degree. Thus the DLTS spectra may show positive signals during the temperature scan if the number of filled electron traps is larger than filled hole traps at the given temperature. It follows that a hole peak may be seen as a minimum in a spectrum with positive ΔC if the defect density is small.

The signals plotted in the figures are quoted as positive and negative numbers of arbitrary units. The relation to the measurement results is 1 arbitrary unit $= 1\times10^{9}$ cm^{-3}, and this density is calculated from $N_t = 2N_d\Delta C/C_0$ where N_d is the doping concentration, ΔC is the DLTS capacitance signal and C_0 is the junction capacitance at the DLTS reverse bias. However, in order to find the correct defect density we also have to include various correction factors, which require additional measurements. These correction factors and their calculation have been discussed at length in another paper written by us [15]. In addition the ΔC used should be corrected if $\Delta C = 0$ does not correspond to the true zero-hole signal.

The measured DLTS signal is due to the sum of all the defects in the depletion zone, and by calculating the defect density it is assumed that the density is constant throughout the measured region. If this is not true we will obtain some average defect density. When measuring hole traps we measure the whole region from the pn junction to the depletion zone edge.

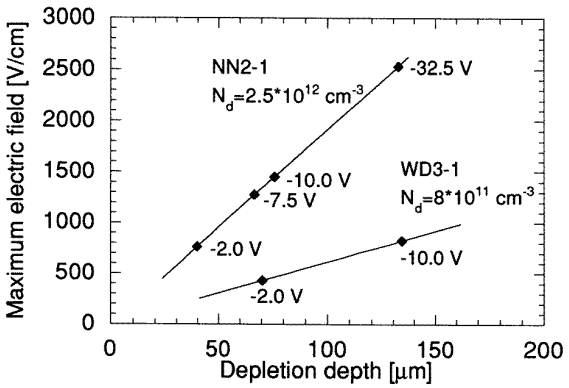

Figure 1. Maximum electric field as a function of depletion depth for the two diodes used in this investigation. The reverse bias voltages used are indicated.

3. DLTS measurements and discussions

The DLTS electron spectra show one electron peak in diode WD3-1 around 100 K. Results for this peak have been presented elsewhere and will not be discussed here [11]. The electron spectra appear constant after repeated scans.

The two diodes used in this investigation had different doping concentrations. As a consequence the depletion depth and the maximum electric field will be different for the same bias voltage. This is illustrated in figure 1, where the maximum electric field versus depletion depth has been plotted for the two doping concentrations. The reverse bias voltages used in this work have been indicated on the curves.

In the following we will show the results of the DLTS hole trap scans and discuss the implications. First the metastable behaviour of the peaks will be discussed, and afterwards the spatial distribution of the defects. Finally we will discuss the origin and possible identifications of the various peaks.

3.1. Metastability

In the DLTS hole trap spectra we observed two peaks after repeated DLTS measurement scans with suitable reverse bias. We have labelled the peaks H1 and H2 with peak temperatures at 100–130 and 180 K respectively. Figure 2 illustrates that the DLTS signal increases in consecutive scans. This measurement was performed on diode NN2-1 at -10 V reverse bias. The measurement series was started at 300 K, thus the odd-numbered scans are performed with decreasing temperature and the even-numbered ones with increasing temperature. Scan 1 (the curve labelled 1(-10 V)) yields positive signals but with a small dip at 180 K. In scan 2 the dip results in a negative signal at the H2 peak temperature. Then in scan 3 there are clearly two hole peaks present, the one at lower temperature called

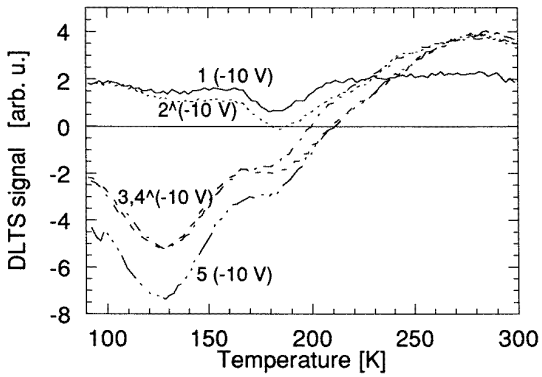

Figure 2. DLTS signals in consecutive scans on diode NN2-1 at −10 V reverse bias.

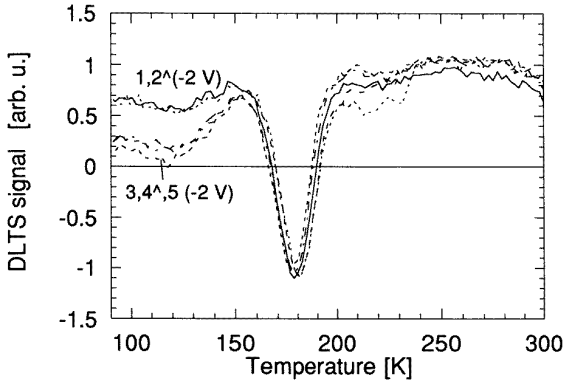

Figure 3. DLTS signals in consecutive scans on diode NN2-1 at −2 V reverse bias.

H1. Scan 4 is similar to scan 3 and in scan 5 the signals have increased further. Figure 3 shows the hole trap spectra due to repeated DLTS scans on the same diode with −2 V reverse bias. The peak named H2 is observed and does not change, while the H1 signal is small and changes very little for repeated scans.

If the diodes are kept at room temperature without bias for some time the measurement series shown in figures 2 and 3 can be repeated with the same result. We suggest that the alternation between low and high peak signals is caused by one or more metastable defects which has one configuration that gives rise to the H1 peak and one configuration which is not visible in our DLTS spectra. Further we suggest that the transition to the visible configuration is dependent upon an electric field in the diode. The small hole signal in the first scan indicates that there is a time constant involved in the change of configuration, and that a longer time with electric field is needed for the change. In addition a certain thermal energy is necessary, so negligible reconfiguration takes place at low temperature. The H1 peak is hardly visible at small reverse bias, which we interpret as indicating a small defect density close to the pn junction. From other measurements to be shown later we observe small hole signals when the bias voltage is large, and we consider this as an indication for a small defect density deep in the bulk as well.

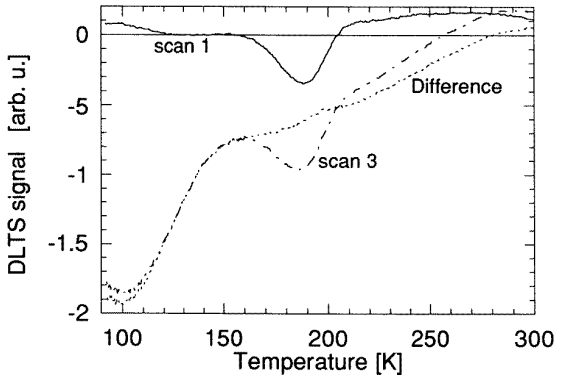

Figure 4. The first and third scans after bias turn-on of −10 V on diode WD3-1, and the difference between the signals of the two scans.

The spectra shown in figure 4 are from measurements on diode WD3-1 with −10 V reverse bias. The first and the third DLTS scans performed after bias voltage turn-on are shown together with the difference between the two scans. This difference is due to metastable defects which have appeared after the first scan. We observe that this spectrum does not contain a peak at 180 K, and we therefore conclude that the defect giving rise to the H2 peak is not metastable. The metastable H1 peak has a long tail towards higher temperatures which overlaps the H2 peak temperature and therefore the signal at 180 K will increase as the metastable defects emerge. Because of the slope of the high-temperature tail, the emerging metastable defects will in some scans cause a shift in the temperature where the minimum occurs around H2.

Based on our measurements we have developed a model for the metastable defects. In this model the defects have a non-uniform density with a peak at some distance from the pn junction and a small or negligible density close to the junction and deeper in the bulk. The fraction of the defects in the visible configuration depends on the electric field across the junction. Figure 5 shows a schematic illustration of our model. In this simplified illustration we have pictured the metastable defect(s) with a constant density at some depth from the pn junction and zero density elsewhere. The hatched part shows the fraction of the defects in the visible configuration. A sketch of the diode indicating the depletion depth is also included, and an indication of the measured DLTS peak signal in the various situations. The various parts of figure 5 show the presumed situations when the reverse bias voltage is varied. Figures 5(a) and (b) corresponds to the situations shown in figure 2. The other figures show situations corresponding to measurements to be presented.

Figures 6–9 show the DLTS spectra from a series of measurement scans on the diodes WD3-1 and NN2-1. In these measurement series the reverse voltage was changed at 90 K between some of the scans. Two reverse voltages were used in each series and these were −2 and −10 V, and −7.5 and −32.5 V. −7.5 and −32.5 V in diode NN2-1 corresponds to −2 and −10 V in WD3-1 with regard to depletion depth.

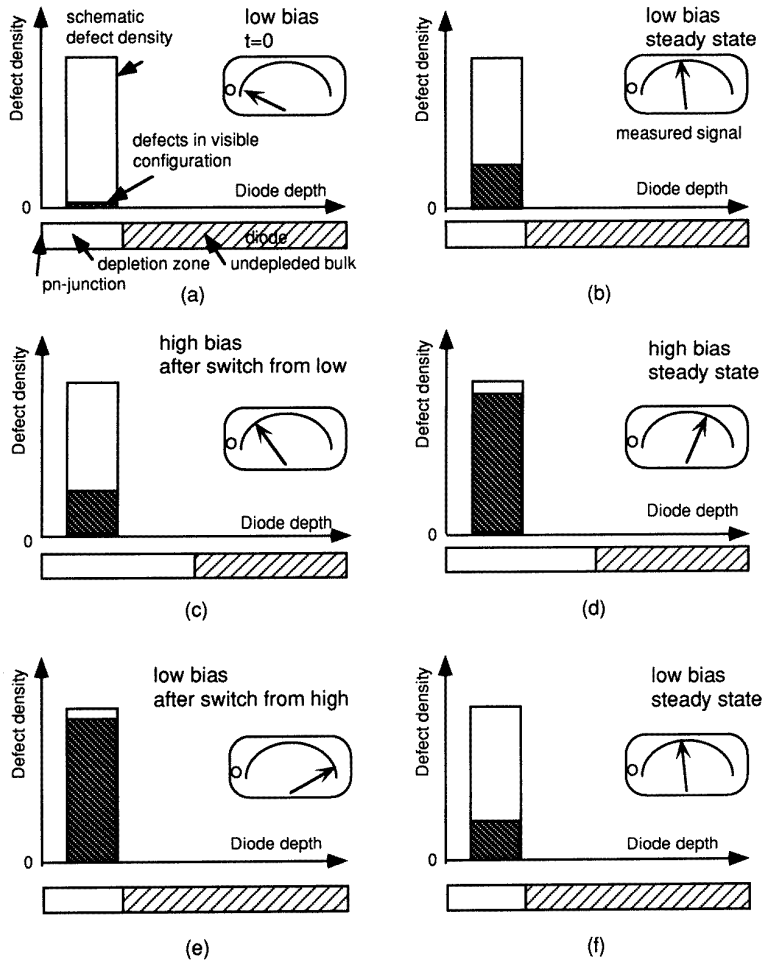

Figure 5. A schematic illustration of the measured DLTS signal and the 'visible' defect concentration for the metastable defect(s) at various biases. (a) Immediately after low-bias turn-on. (b) 'Steady state' at low bias. (c) Immediately after increase from low to high bias. (d) 'Steady state' at high bias. (e) Immediately after decrease from high to low bias. (f) The same as (b).

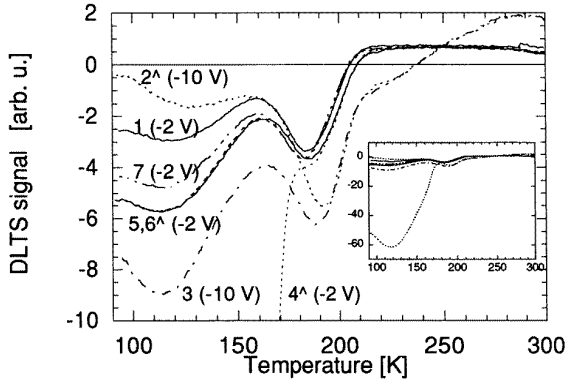

Figure 6. Consecutive DLTS scans from diode WD3-1 with −2 and −10 V reverse bias.

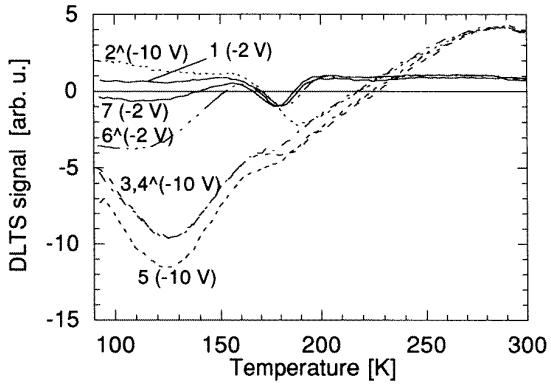

Figure 7. Consecutive DLTS scans from diode NN2-1 with −2 and −10 V reverse bias.

The DLTS signal measured after an increase from low to high bias can be observed in scans 2, 2 and 4 of figures 6–8 respectively. There is a reduction in the hole signal around the H1 temperature compared to the previous scan. This signal reduction is explained as follows. The measured signal depends on the average density in the

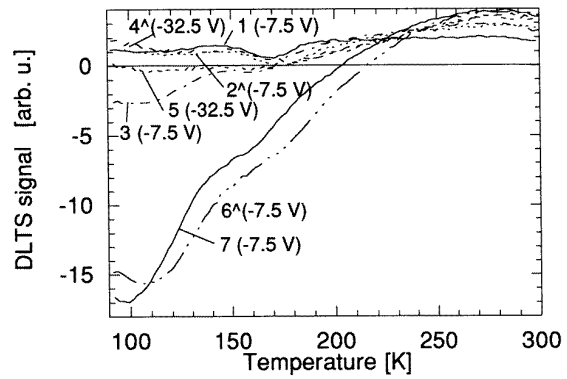

Figure 8. Consecutive DLTS scans from diode NN2-1 with −7.5 and −32.5 V reverse bias.

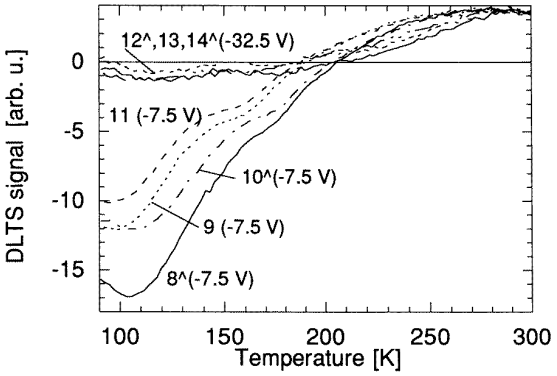

Figure 9. Consecutive DLTS scans from diode NN2-1 with −7.5 and −32.5 V reverse bias. This was performed immediately after the measurement series shown in figure 8.

depletion zone and when the depletion zone increases at low temperature the defects in the extended zone will not participate until they have been transformed to the visible configuration. The reconfiguration is inhibited at low temperature. This corresponds to the transition between the situations illustrated in figure 5(b) and (c). As the temperature increases (scans 2, 2 and 4 of figures 6–8) the defects gain sufficient energy to change configuration and the hole signals increase. This process begins below the H2 peak temperature.

In the next scan (scans 3, 3 and 5) the signals of the H1 peak and the high-temperature tail have increased substantially and small increments are seen in some of the subsequent scans. This corresponds to the transformation from figure 5(c) to (d). The signals increase due to the higher electric field which causes a larger fraction of the defects to be transformed to the visible configuration. In figures 6 and 7 the H1 peak has a larger signal at high bias than at low bias. However, in figure 8 the signal in scan 5 with high bias is smaller than in scan 3 at low bias. Thus the average density in the depletion zone is smaller for −32.5 V than −7.5 V for NN2-1. We suggest that this is due to a small defect density in the extended depletion zone for this diode.

The changes in the DLTS signal after a decrease from high to low bias are observed in scans 4, 6 and 6 of figures 6–8 respectively. This results in a large increase in the H1 signal in figures 6 and 8, where the low-bias depletion depth is approximately 70 μm. This corresponds to the situations illustrated in figure 5(d) and (e). The depletion zone decreases and the defects previously transformed to the visible configuration by the high electric field remain in this configuration as long as the temperature is low. Thus the signal increases. In figure 7 where the low bias depletion depth is approximately 40 μm the signal decreases. We interpret this as being due to a small defect density in this depletion zone.

In figure 6 (diode WD3-1) we observe that the H1 signal measured in the next scan (scan 5) has decreased by 90%, whereas in scan 7 of figure 8 we observe a shift in the H1 peak temperature and a small increase of the peak signal. In the subsequent scans (scans 8 to 11) shown in figure 9, performed immediately after the scans in figure 8, a small decrease is observed. These different measurement results may be explained by the differences in the electric fields in the diodes as illustrated in figure 1. The maximum electric field in diode NN2-1 is higher for −7.5 and −32.5 V than the fields in diode WD3-1. It is likely that the field at −7.5 V in diode NN2-1 is sufficient to keep a large fraction of the defect(s) in the visible configuration. The field in diode WD3-1 can only keep a small fraction in the visible state, hence the large decrease of the signal.

It may be noticed that the transformation back to the invisible state occurs at a lower temperature than the H2 peak when the electric field is reduced. This can be seen from figure 6 where scan 4 is the first scan after bias voltage reduction. The H1 peak increases substantially when switching the bias ($3 \rightarrow 4$) but the signal is reduced to the size obtained in the other low-bias scans (scans 5–7) at the H2 peak temperature.

Initial investigations on the temperature stability of the detects have been performed. Two diodes from the same wafer as NN2-1 were annealed at 300 °C in N_2 ambient for 20 min. Subsequent DLTS results were similar to the results shown for the non-annealed diodes NN2-1 and WD3-1.

3.2. Defect density depth distribution

The non-uniform density can be deduced from the variation in the peak signal for various reverse voltages. A good illustration is given by scans 4, 6 and 6 in figures 6–8 which were discussed in the previous section. From these scans, performed after bias voltage reduction we may conclude that the defect density is significantly higher between 40 and 70 μm than below 40 μm (figure 7), and that the average defect density between 0 and 130 μm is less than the average density between 0 and 70 μm (figures 6 and 8). With regard to the density below 40 μm our conclusion is strictly speaking only valid for diode NN2-1. DLTS measurements with a depletion depth of 40 μm on diode WD3-1 are not possible due to the low doping concentrations.

We have used the variation in the measured signal as an argument to show that the defect density decreases deep

in the diode. However, this is not necessarily correct and a further justification of this hypothesis is needed. The holes injected across the junction diffuse and recombine, which results in a decreasing hole density, with distance from the junction. The fraction of the defects filled with holes depends on the hole density, and if the hole density at the end of the reverse bias depletion zone is too small the filling fraction over the depletion zone will vary. To avoid this problem the minority carrier diffusion length should be substantially longer than the reverse bias depletion depth. The minority carrier lifetime was measured using the ramp recovery method described by Berz [16]. To calculate the lifetime from this measurement one must assume that the lifetime is constant throughout the wafer. This is not true when the defect density is not uniform, and by performing measurements at various reverse biases somewhat different lifetimes were measured. Our results indicated an average lifetime of the order of 100 μs at 110 K, which corresponds to a minority carrier diffusion length of 700–800 μm. This should be compared to the 135 μm deep depletion zone at the highest reverse bias. In conclusion we find that the diffusion length is sufficient to ensure a reasonably uniform filling fraction of the defects in the depletion zone.

In the following we present a possible explanation for the defect density distribution. It is well known that in silicon wafers with high oxygen concentration such as Czochralski grown wafers a denuded zone is formed close to the surface when the wafers are heated to high temperatures. Nauka and co-workers have investigated the effect of this process on floatzone silicon and found that despite the low oxygen concentration a denuded zone is formed [17, 18]. They found that the depth of the denuded zone varied between 2 and 100 μm depending on the ambient in the high-temperature step. The largest depth was found for $O_2 + HCl$, and the smallest for O_2. They have suggested that the denuded zone is formed by out-diffusion of interstitial silicon and that the difference due to various ambients is due to whether the process causes 'injection' or 'extraction' of interstitials at the $Si–SiO_2$ interface.

Our first oxidation process consists of oxidation at 1100 °C in different steps using $O_2 + HCl$, $O_2 + H_2$ and N_2. We speculate that it will result in a denuded zone in accordance with the results of Nauka *et al*. We suggest that defects beyond the denuded zone will getter impurities during the following processing steps. If the getter zone functions as a sink for impurities the concentration of mobile impurities will decrease deep in the bulk.

It should be added that drift of defects in the depletion zone could play a part in the measurement results. Further and other measurements are needed to find out whether this may be an important process for these defects.

3.3. Peak identities

The signature of H2 is $E_v + 0.31$ eV for the activation energy and 1×10^{-15} cm^{-2} for the apparent capture cross section. This signature was found by measurements on NN2-1 using -2 V as reverse bias. The metastable defects were negligible in this diode at this low reverse bias. This signature agrees well with the data found by Indusekhar and Kumar for a nickel related defect [19].

We have observed that the peak which we have called H1 moves in temperature between 100 and 130 K. This indicates that the peak consists of more than one metastable configuration of the same defect or of two or more different metastable defects. Both possibilities may be true. At this stage we have not been able to determine the conditions which cause the peak shift.

In addition to the H1 peak there is also a significant background extending over most of the lower half of the bandgap. We suggest that this is due to a number of closely spaced energy levels which arise when the gettering site is being decorated by impurities. If the metastable behaviour is due to properties of the gettering site itself, the defect configuration will change in the same manner even if different impurities have been gettered. The different energy levels may also be caused by different configurations of the same defect with a decreasing filling fraction as the energy levels move closer to mid-gap.

4. Summary and conclusions

We have shown that these high-resistivity floatzone diodes contain defects which are driven into a metastable state by applying an electric field across the diode. The metastable states (one or more) act as hole traps in DLTS measurements. The measurements are in agreement with a model where the fraction of defects in the metastable state depends on the field strength. Further, the defect density varies with depth with a peak somewhere between 50 and 100 μm from the pn junction, and a small or negligible density closer to and further from the junction. We have suggested that these defects are formed by internal gettering of impurities in the bulk beyond the denuded zone.

Acknowledgments

The author would like to express her gratitude to Dr Terje Finstad for valuable suggestions and discussions during this work. Thanks are also due to SINTEF for use of silicon processing facilities and various measurement equipment, and TeleNor Research and Development for use of their DLTS equipment.

References

[1] Benton J L and Levinson M 1983 *Mater. Res. Soc. Symp. Proc.* vol 14 (Pittsburgh, PA: Materials Research Society) p 95
[2] Chantre A and Bois D 1985 *Phys. Rev.* B **31** 7979
[3] Chantre A and Kimerling L C 1986 *Appl. Phys. Lett.* **48** 1000
[4] Song L W, Benson B W and Watkins G D 1986 *Phys. Rev.* B **33** 1452
[5] Zhan X D and Watkins G D 1991 *Appl. Phys. Lett.* **58** 2144
[6] Zhan X D and Watkins G D 1993 *Phys. Rev.* B **47** 6363
[7] Song L W, Zhan X D, Benson B W and Watkins G D 1988 *Phys. Rev. Lett.* **60** 460
[8] Song L W, Zhan X D, Benson B W and Watkins G D 1990 *Phys. Rev.* B **42** 5765
[9] Benton J L 1989 *J. Electron. Mater.* **18** 199
[10] Nakashima H, Sadoh T and Tsurushima T 1993 *J. Appl. Phys.* **73** 2803

[11] Avset B S 1997 *Nucl. Instrum. Methods* A accepted for publication
[12] Lang D V 1974 *J. Appl. Phys.* **45** 3023
[13] Blood P and Orton J W 1992 *The Electrical Characterization of Semiconductors: Majority Carriers and Electron States* (London: Academic)
[14] Bio-Rad Microscience Ltd, Bio-Rad House, Marylands Avenue, Hemel Hempstead, Hertfordshire HP2 7TD, UK
[15] Avset B S *Department of Physics, University of Oslo Report Series* UiO/PHYS/96-07
[16] Berz F 1980 *Solid State Electron.* **23** 783
[17] Nauka N, Lagowski J, Gatos H C and Li C-J 1985 *Appl. Phys. Lett.* **46** 673
[18] Nauka K, Lagowski J, Gatos H C and Ueda O 1986 *J. Appl. Phys.* **60** 615
[19] Indusekhar H and Kumar V 1987 *J. Appl. Phys.* **61** 1449